



UiT Norges arktiske universitet

Model Calculations on the Influence of Charged Mesospheric dust on the Incoherent Radar Spectrum

Tinna Gunnarsdóttir¹, Ingrid Mann¹ and Wojciech Miloch²

¹UiT Arctic University of Norway, Faculty of Science and Technology, Department of Physics and Technology, Norway (tinna.gunnarsdottir@uit.no)

²University of Oslo, The Faculty of Mathematics and Natural Sciences, Department of Physics

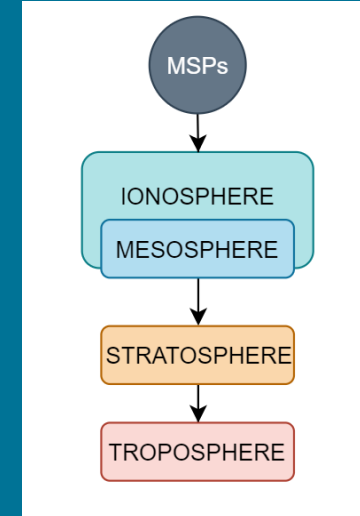


Overview & Background

- Detection of charged dust in the incoherent scatter spectrum observed with radars has previously been proposed and examined to some degree. These dust particles are of nanometer size and reside at mesospheric altitudes due to incoming ablating meteors.
- We here present model calculations that simulate the incoherent scatter spectrum including dust with a size distribution assuming a set of size bins.
- We investigate the influence of different sizes and number densities on the radar spectrum. A charging model is used to model the most probable charge and altitude dependence.
- We discuss the influence of the dust on the scatter spectrum for different ionospheric conditions during the year assumed for the location of the future EISCAT_3D site.

Dust in the Mesosphere

- Meteors and meteorites ablate in the mesosphere at altitudes of 70-110 km.
- This material is then thought to re-condense into Meteoric Smoke Particles. Which are Nanometer sized dust particles.
- They reside in the mesosphere, but as they grow, descend lower in the atmosphere and influence processes in the stratosphere.
- Eventually they deposit on the ground.



Dust Detection with Incoherent Scatter Radars

Cho et al. (1998) formalism:

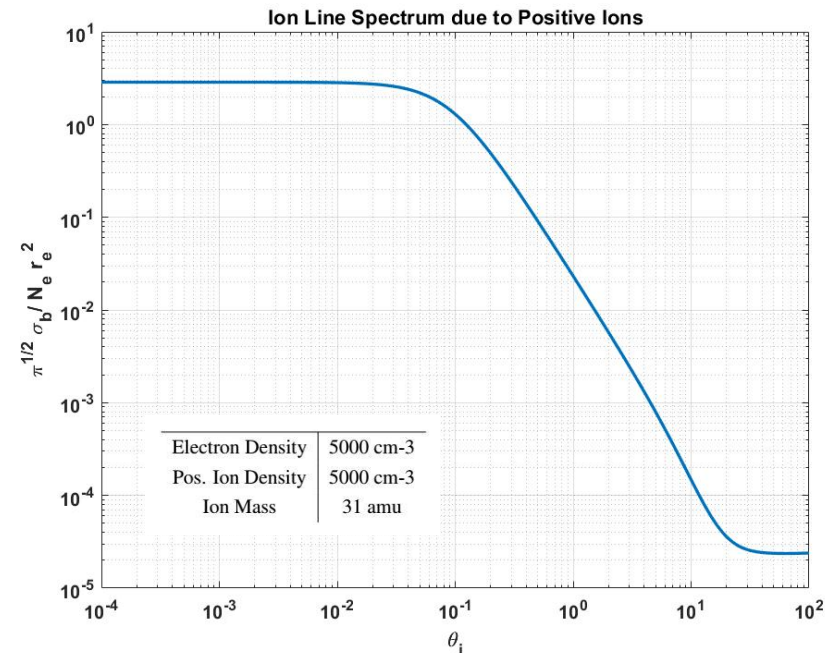
Backscatter cross section accounting for dust interactions:

$$\sigma_b(\omega_0 + \omega)d\omega = \frac{r_e^2 N_e}{\sqrt{2}\pi\omega} \left| \frac{1}{\alpha_e^2 + z_e \left(\sum_{s \neq e} \frac{\alpha_s^2}{z_s} \right)} \right|^2 \times \left(\left| 1 + \sum_{s \neq e} \frac{\alpha_s^2}{z_s} \right|^2 z_e + \frac{\alpha_e^2}{T_e} \sum_{s \neq e} T_s \frac{\alpha_s^2}{z_s^*} \right)$$

Here ω_0 is the radar frequency and ω is the doppler frequency shift
 Subscript *e* denotes electrons and subscript *s* denotes positive and negative ions as well as positive and negative dust components.
 - α depends on the **Debyelength** for each constituent and the backscatter radar **Bragg wavenumber**.
 - z depends on, among others, the **normalized frequency** of each constituent as well as the **normalized collision frequency** with the neutral gas.

- A basic figure is given to the right which depicts the spectrum with only positive ions and electrons present. This spectrum is referred to as σ_b in later plots.
- This part of the incoherent scatter spectrum is known as the ion line which forms because of the coupling between the electrons and ions and the ion-acoustic wave conditions present in the mesosphere.

- Cho et. Al. (1998) developed a description of the incoherent scatter spectrum in the presence of charged dust particles. (equation to the left).
- Our calculations of the spectrum follow an implementation of this model by Strelnikova et al (2007) and Teiser (2013) and extend this by including a number of different dust sizes and charge that later can be used for larger data sets.



Normalised Frequency:

$$\theta_s = \frac{\omega}{\sqrt{2}k v_s}$$

Mean thermal velocity:

$$v_s = \sqrt{\frac{k_B T_s}{m_s}}$$

Figure – So called ion line part of the spectrum containing electrons and positive ions.

Constituent-Neutral Collision Frequencies

- The collision frequency between electron, ions or dust with the neutral gas is important when looking at the spectrum influence.
- In the equation box to the right the different collision frequencies are shown. First the neutral-electron interaction and then the polarization coll. freq. which is valid for ions as well as for the smaller dust sizes (<0.5 nm). The last is the hard-sphere coll. freq. which is valid for larger dust sizes (Cho et al. 1998).

Constituent-Neutral Collision Frequency:

$$v_e = (3.78 \times 10^{-11} T_e^{1/2} + 1.98 \times 10^{-11} T_e) N_n$$

$$v_{polar} = 2.59 \times 10^{-9} \frac{N_n}{M_s^{1/2}} \sum_t F_t \left(\frac{M_{nt} \chi_{nt}}{M_s + M_{nt}} \right)^{1/2}$$

$$v_{hSph} = \frac{8(r_s + r_n)^2 N_n}{3(m_s + m_n)} \left[\frac{2\pi k_B m_n (m_s T_n + m_n T_s)}{m_s} \right]^{1/2}$$

- Electron-Neutral Collision Frequency
- Polarization Collision Frequency
- Hard-Sphere Collision Frequency

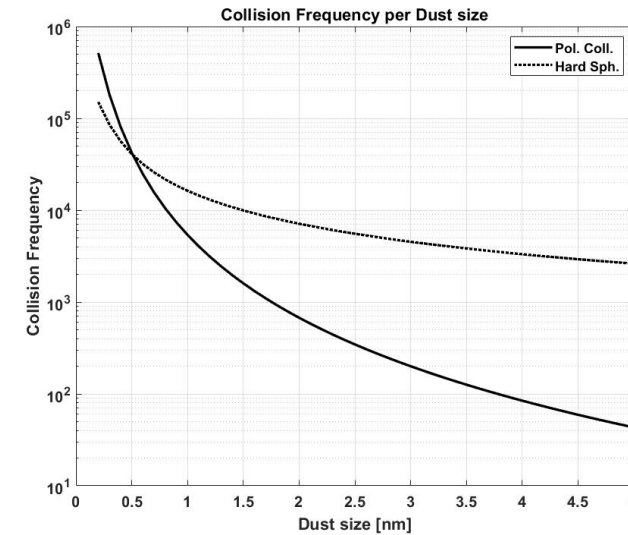


Figure – Comparison of Polarization and Hard-sphere neutral-dust collision frequencies.

Collision Frequency for Different Dust Sizes

- The choice of collision frequency is very important as it influences the spectrum differently with different size
- Cho et al. (1998) proposed using the highest collision frequency for each dust-size.

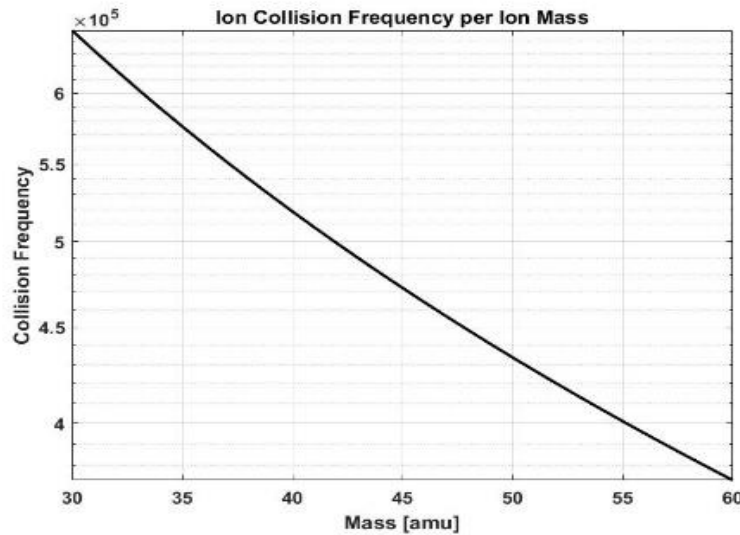


Figure – Ion neutral collision frequency as a function of ion mass.

Effect of varying the ion mass

- Increasing the ion mass decreases the Collision frequency with the neutral gas.
- However the dependency of the spectrum on the collision-frequency is complex.
- The decrease is not large enough to influence the spectrum in a noticeable way.

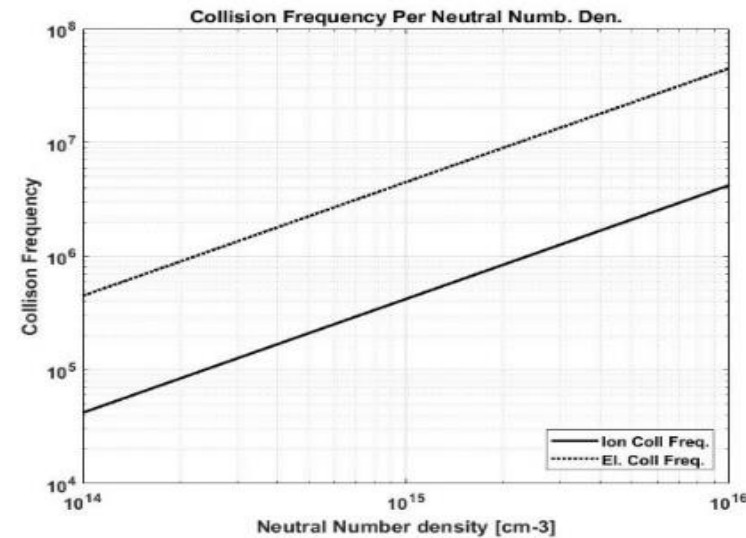


Figure – Collision frequency of electron and ions with varying neutral gas density.

Collision Frequency variations with Neutral Density

- Both collision frequencies increase with increasing neutral density
- Accurate estimate of the neutral density is important since the spectrum can vary a lot with a factor difference in the collision frequency.

Influence on Spectrum without Dust

- On the right is shown how the temperature influences a spectrum with no dust present.
- An accurate temperature at the time of measurements is important so as to not confuse with dust signature.

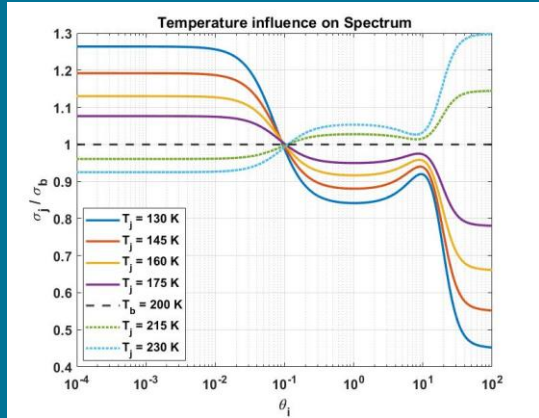


Figure – Ratio of spectrum with varying temperature compared with 200 K.

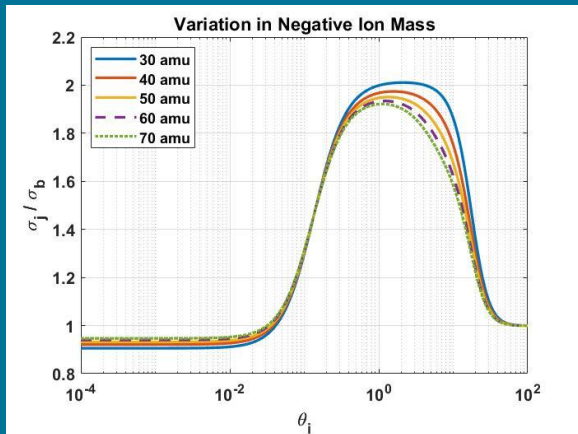
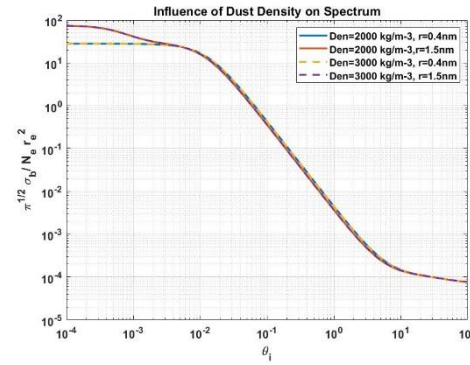


Figure - Ratio of keeping the positive ion mass constant and varying the negative ion mass from 30 to 60 amu. $N_{pi} = 7500 \text{ cm}^{-3}$ and $N_{ni} = 2500 \text{ cm}^{-3}$.

- Including the correct amount of negative ions can be a challenge.
- This is both important for the overall charge balance as well as interpreting the amount of dust present.

Comparison of different dust mass density



- Composition, number density and dust size can all influence the spectrum – but in different ways.
- Varying the dust mass density does not seem to have a large influence

Figure – Varying the dust mass density for two dust particle sizes

Comparison of small and large particle sizes

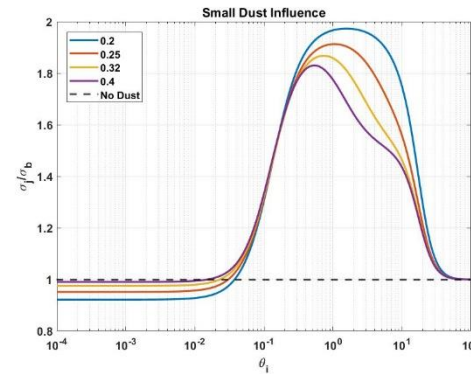


Figure – Varying the dust mass density for two dust particle sizes

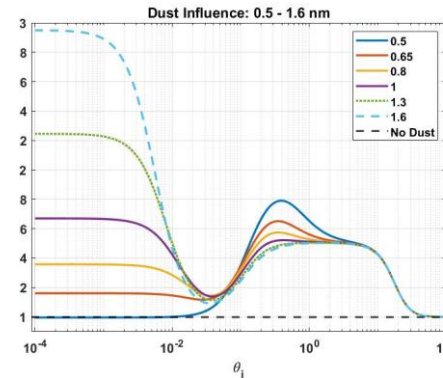


Figure – Dust sizes in range 0.5-1.6 nm

- Dust smaller than 0.5 nm mainly influences the spectrum in the higher part of the frequency range
- Larger dust particles with same number densities influence the spectrum greatly. This is however unphysical as most models have shown much greater abundance in the smaller dust size region.

Comparison of different dust Number Densities

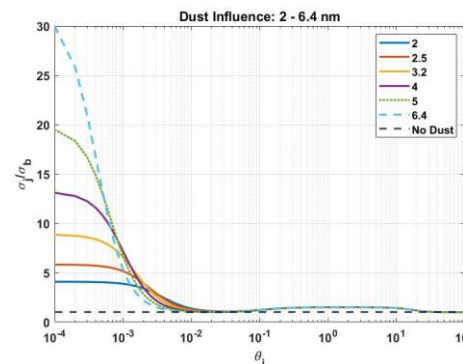


Figure – Dust sizes in range 2-6.4 nm

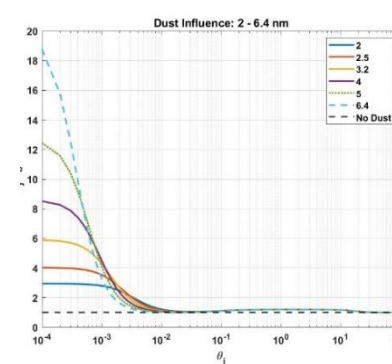


Figure – Dust sizes in range 2-6.4 nm

- To the left the spectrum is shown for large dust sizes with two different number density distributions for each size.
- This shows that the combination of dust size and number density is extremely important.

Dust influence

- All dust comparisons are done with a dust number density of 2500 cm^{-3} except the bottom right figure which has a number density of 1000 cm^{-3} .

Dust Size Distributions

- Dust number density per size is important since the spectrum is influenced differently for each dust size
- The total number density of dust is possibly rather large. However the amount that is negatively or positively charged is debated.
- Here we have employed the number densities from model by Megner et al. (2006) and the total percentage that is charged is from charging model of Baumann et al. (2015).

Smaller Dust sizes

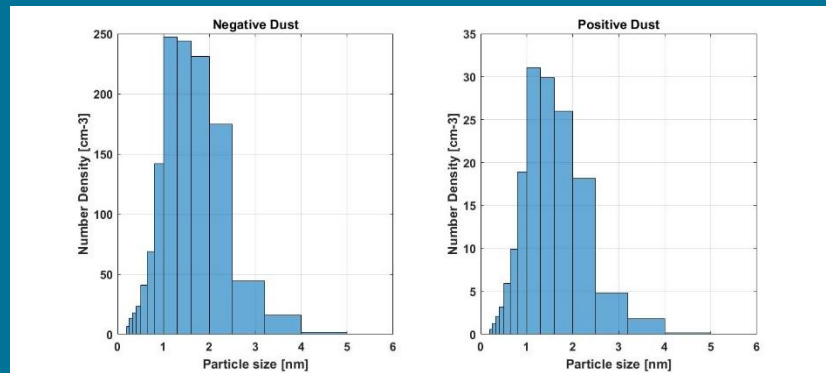


Figure - Dust number density per dust size given in a histogram below. Data from Baumann et al(2015) and Megner et al (2006)

Dust	Total Number Density [cm-3]	% of Total
Neutral Dust	3.6220e+04	96.21
Negative Dust	1.2730e+03	3.38
Positive Dust	153.7178	0.41

Atmospheric Conditions – Skibotn Location

- Models (ref. 6) and 7)) used to determine the local conditions at Skibotn site (where EISCAT-3D will be located)
- The temperature and neutral density to the right are taken at each month at 12:00 hr and the electron density data below is also taken at taken at 12:00 local time and represents average values at the Skibotn location.
- Temperature shows the warmer winter conditions and colder summer conditions in the mesosphere.
- The neutral density influences the spectrum by way of collision frequency with all constituents. The figure to the right shows a general increase in neutral density during summer. With the lower altitudes (60-70 km) having almost a factor difference in the total density.

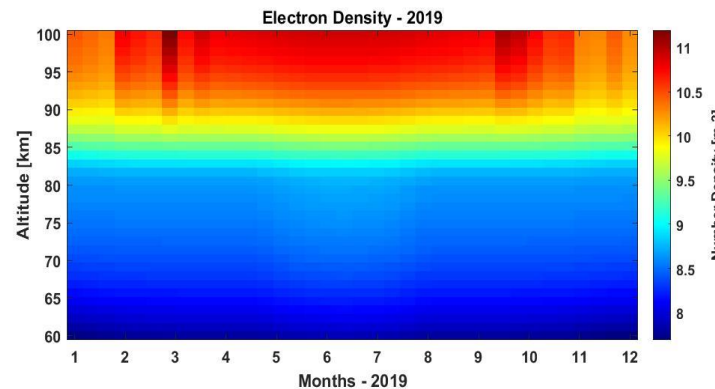


Figure – Electron density for each month for year 2019. Data from IRI- model in ref 7).

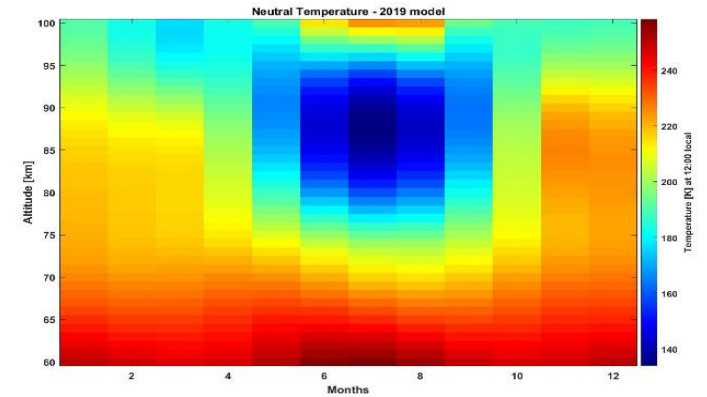


Figure – Temperature data for all months in 2019. from NRLMSISE-00 model

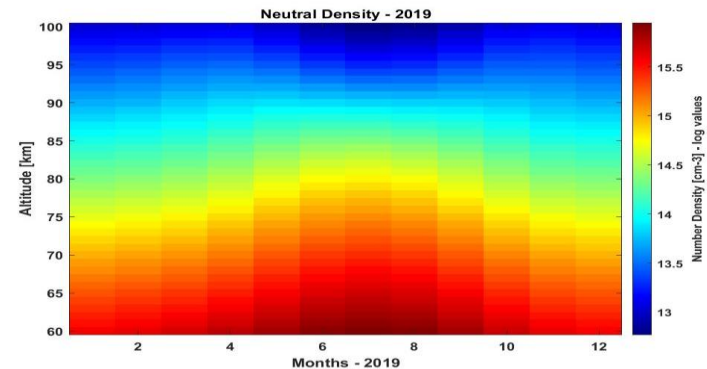


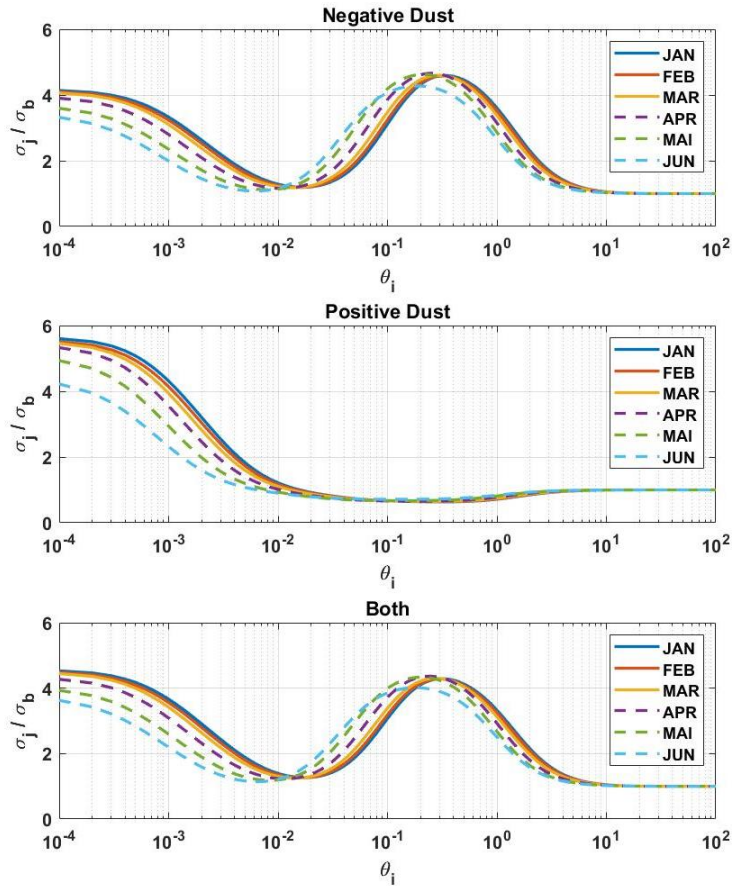
Figure – Neutral gas total number density of the main constituents from NRLMSISE-00 model. For all months in 2019.

•This can then be replaced with more detailed modeled conditions using global atmospheric circulation model like WACCM

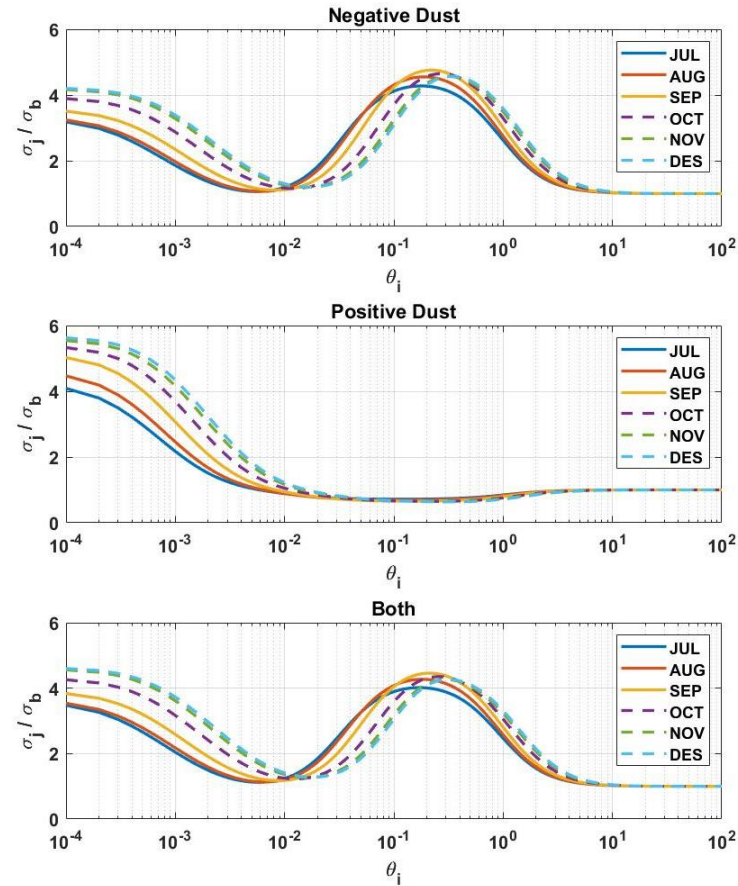
•Data is used for each of these values to roughly represent plausible values at altitude of 79 km used in the data analysis on the next slide.



Dust Influence on Spectrum - 2019 data from model



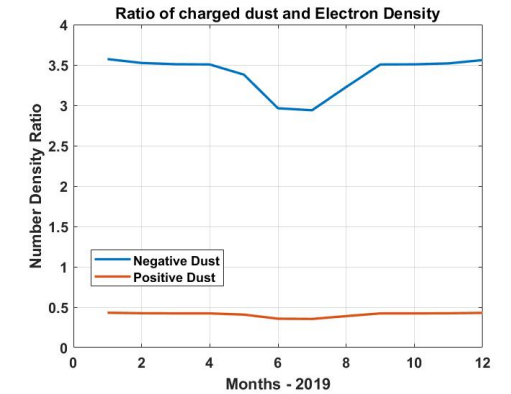
- **Only Negative Dust** – Winter conditions show higher spectrum ratio in the lower part of the normalized frequency. In the higher frequency part the ratio is lowest for June to August part, corresponding with lower ratio of negative dust to electrons in the summer. Thus choosing winter conditions with highest dust to electron density ratio would be optimal for best dust detection.



- **Only Positive Dust** – The ratio of the spectrum in the lower part of the normalized frequency is much higher than the negative ratio even though the positive number densities are much lower. This is due to the fact that the ratio of positive ions to electrons becomes smaller for positive dust due to charge neutrality condition must be kept. This causes a large spectrum ratio, but only in the lower part of the normalized frequency. This part of the spectrum is more difficult to detect with the EISCAT radar system.

Left Figure – Simulated spectrum using data from previous slides for each month in 2019 at 12:00 local time.

Right Figure – Ratio of total dust density to total electron density per each month for 2019. For both positive and negatively charged dust.



- The spectrum has been simulated for each month of 2019. Using average atmospheric conditions and dust size and number density from previous slide.
- Each monthly spectrum is divided by the spectrum for only positive ions present.

Possible dust signatures at Skibotn location

- **Negative and Positive dust** – A combination of both charge states shows that the small number density used for the positive dust does not seem to matter much in terms of increasing the spectrum ratio. It is only slightly higher than the spectrum with only negative dust and mainly influences the lower part of the normalized frequency. Showing that optimal conditions would be with as much negative dust as possible in order to detect the dust signature above the EISCAT radar system resolution.

Future work will address:

- collision frequencies between dust, plasma and neutrals and their influence on the ion line spectrum.
- the influence of multiple dust charges on the ion line spectrum
- the influence of negatively charged dust on the ion line spectrum and possible detection methods using EISCAT-3D radar system

Acknowledgements

- *This work is funded by the Norwegian Research Council – Project NRC-275503*

References

- 1) Baumann, C., Rapp, M., Anttila, M., Kero, A., & Verronen, P. T. (2015). Effects of meteoric smoke particles on the D region ion chemistry. *Journal of Geophysical Research: Space Physics*, 120(12), 10-823.
- 2) Cho, J. Y., Sulzer, M. P., & Kelley, M. C. (1998). Meteoric dust effects on D-region incoherent scatter radar spectra. *Journal of atmospheric and solar-terrestrial physics*, 60(3), 349-357.
- 3) Hagfors, T. (1992). Note on the scattering of electromagnetic waves from charged dust particles in a plasma. *Journal of atmospheric and terrestrial physics*, 54(3-4), 333-338.
- 4) Megner, L., Rapp, M., & Gumbel, J. (2006). Sensitivity of meteoric smoke distribution to microphysical properties and atmospheric conditions.
- 5) Strelnikova, I., Rapp, M., Raizada, S., & Sulzer, M. (2007). Meteor smoke particle properties derived from Arecibo incoherent scatter radar observations. *Geophysical Research Letters*, 34(15).
- 6) NRLMSISE-00 Atmosphere Model - <https://ccmc.gsfc.nasa.gov/modelweb/models/nrlmsise00.php>
- 7) International Reference Ionosphere - IRI (2016) with IGRF-13 coefficients - https://ccmc.gsfc.nasa.gov/modelweb/models/iri2016_vitmo.php
- 8) Teiser, G. (2013). Zum Einfluss von geladenen Aerosolen auf die inkohärente Rückstreuung von Radarwellen aus der oberen Mesosphäre. Masterthesis – IAP.
- 9) Read more on the EISCAT 3D project: https://uit.no/prosjekter/prosjekt?p_document_id=487937



UiT The Arctic
University of Norway